

## EFFECTS OF VELOCITIES ON Ca II H AND K LINES

K. E. RANGARAJAN, D. MOHAN RAO and A. PERAIAH

### ABSTRACT

Ca II H and K (3908, 3933) and Infrared triplet lines  $\lambda\lambda$  8446, 8502, 8542 were calculated in a very slowly expanding medium. Five level atom with continuum was considered. Radiative transfer equation and statistical equilibrium equations were solved simultaneously in the star's rest frame within the framework of the discrete space theory technique of Grant and Peraiah (1972). Profiles were computed for the systematic expanding velocities 0.0, 0.5 and 1.0 (expressed in mean thermal units). Even though the velocities are small, they seem to affect the shape of the H and K profiles quite considerably. A single emission peak instead of a double peaked emission for the K lines was obtained when  $V=1$ , and at  $\rho=0.79$ . These small velocities do not affect the Infrared triplet lines significantly.

### 1. Introduction

Linsky and Avrett (1970) reviewed theoretical and observational studies of the profiles of Ca II H and K and Infrared triplet lines in the Sun. They took five levels plus continuum as their atomic model to represent Ca II ion. Integral equation approach was used for the calculation of line source function. Complete redistribution was assumed in their computations. Shine *et al.* (1975) studied the effect of partial frequency redistribution on the formation of Ca II H and K lines in the solar atmosphere. They found the P.R.D. results to be in better agreement with observations. The calculations described above were based on the assumption of a static atmosphere. Consequently the computed profiles were symmetric.

Asymmetric profiles with a single peak emission of the K lines were observed at high spatial resolution studies. (Passchoff, 1970). To account for the asymmetric profiles, Athay (1970) assumed velocity fields in the regions of line formation. He concluded that to obtain  $k_{21}$  enhancement, either the layers where  $K_2$  is formed are moving upward with velocities of 3-7  $\text{km s}^{-1}$  or the  $K_3$  layers are moving downward with velocities of 10-20  $\text{km s}^{-1}$  but he tends to favour the second alternative. He assumed a 3 level atom model with continuum. He used the Integral equation technique generalized for a multi-level atom. Recently Baerl *et al.* (1981) used a comoving partial frequency redistribution code to model the outer atmospheres of cool type stars. They obtained a highly asymmetric profile of Ca II K line which agrees with the observation of this line in  $\beta$  Dra.

We investigated the effect of velocities of the order of 2  $\text{km s}^{-1}$  ( $V=0.5$  case) and 4  $\text{km s}^{-1}$  ( $V=1$ ) on H and K and Infra-triplet lines. We extended the formalism of Grant and Peraiah (1972) for the two level atom model to that of five levels with continuum. To solve the radiative transfer equation in the star's rest frame we used Peraiah's code (1978). This code contains the explicit treatment of velocity fields. In section (2) of this paper we give the atomic model chosen and the method of calculation of various rates. We discuss the computational procedure in section (3). Section (4) contains the results.

### 2. Atomic model

The atomic model chosen is represented in figure 1. We took the  $4^2S_{1/2}$  ground level,  $4^2P_{1/2}$  and  $4^2P_{3/2}$  upper levels,  $3^2D_{3/2}$  and  $3^2D_{5/2}$  metastable levels and the continuum. Temperature ( $T_e$ ) and electron number density ( $n_e$ ) distributions for our atmosphere are given in Figures (2) and (3).

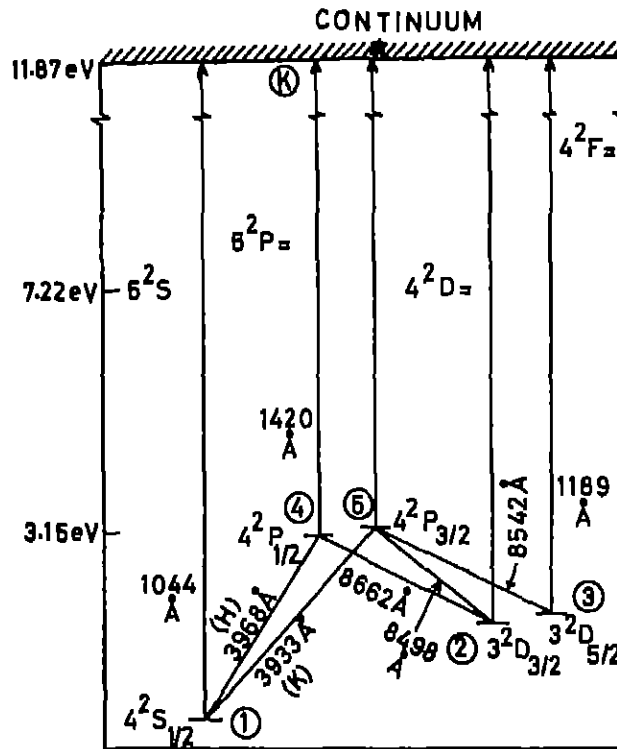


Fig. 1. Energy level diagram for CaII ion with the permitted radiative transitions.

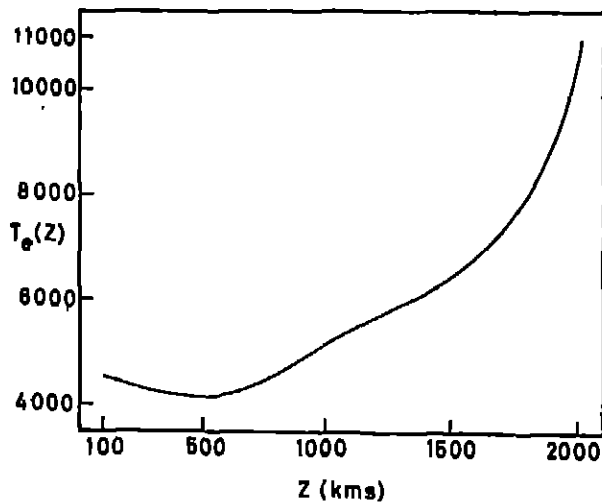


Fig. 2. Temperature  $T_e$  (\*K) distribution of the model chosen is given against the height Z (kms) in the atmosphere.

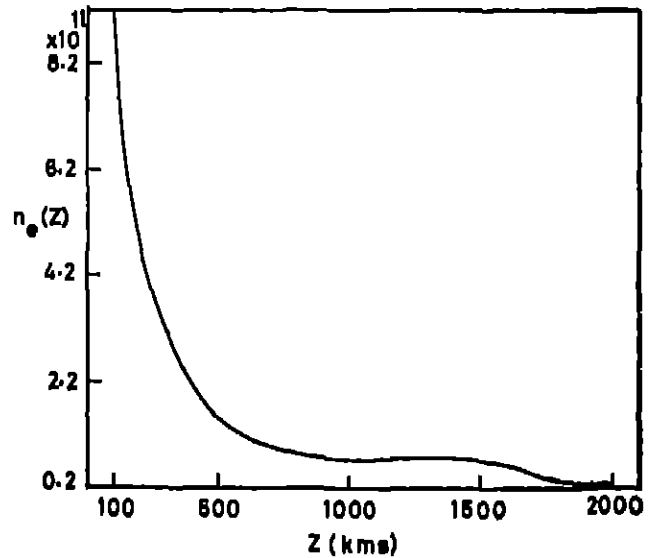


Fig. 3. Electron number density  $n_e$  (per cubic cm) is given with respect to the height Z (kms) in the atmosphere.

Collisional and radiative excitational and de-excitational processes between all the bound levels were considered. Photo-ionization, photo-recombination, collisional ionization and re-combination between the continuum and all the levels were also included.

Photo ionization rates were calculated according to the formula

$$R_{ik} = 4\pi \int_{\nu_i}^{\infty} \frac{d\nu}{h\nu} a_i(\nu) J\nu(Z) \quad (1)$$

$i$  denotes the lower level and  $k$  refers to the continuum.  $Z$  is the height of the atmospheric layer. We approximated  $J\nu(Z) = B\nu(Z)$  where  $B\nu(Z)$  is the Planck function.  $a_i(\nu)$  is the photo ionization cross-section and was taken from Peach's tables (1967). Recombination rates follow from the detailed balance arguments and it is given by

$$R_{ki} = \left(\frac{n_i}{n_k}\right)^* R_{ik} \quad (2)$$

where  $(n_i/n_k)^*$  is the L.T.E. population density ratio obtained from Saha-Boltzmann equation.

Collisional recombination rates were calculated from the formulae given in Linsky's Ph.d. thesis (1969) with the corrections for the inclusion of both the D levels. Detailed balance arguments give the collisional ionization rates by the formula

$$C_{ik} = C_{ki} \left(\frac{n_k}{n_i}\right)^* \quad (3)$$

Spontaneous emission rates (Einstein A values) between the bound levels were taken from the Wiese tables. Collisional excitation and de-excitational rates were calculated according to Giovanelli (1967). Multiplet relations were used to get the rates for the sub levels. To calculate the fine structure transition rates  $C(4^2 P_{3/2} - 4^2 P_{1/2})$  and  $C(3^2 D_{3/2} - 3^2 D_{1/2})$ , Dumont's (1967) cross sections were used and they were derived by treating the collisions to be elastic and collisions with protons to be dominant.

The total number density of  $\text{Ca}^+$  ion was assumed to be  $10^7$ .

### 3. Computational procedure

The equation of transfer is given by

$$\mu \frac{\partial I}{\partial z}(x, \mu, z) = K_L(z) [\beta + \phi(x, \mu, z)] [S(x, \mu, z) - I(x, \mu, z)] \quad (4)$$

and for the oppositely directed beam

$$-\mu \frac{\partial I}{\partial z}(x, -\mu, z) = K_L(z) [\beta + \phi(x, -\mu, z)] [S(x, -\mu, z) - I(x, -\mu, z)]$$

where  $I(x, \mu, z)$  is the specific intensity at an angle  $\cos^{-1} \mu$  ( $\mu \in [0, 1]$ ) at the point  $Z$  and frequency  $X = (\nu - \nu_0)/\Delta$ ,  $\Delta$  being some standard frequency interval. The quantity  $\beta$  is the ratio  $K_c/K_L$  of opacity due to continuous absorption per unit interval of  $X$  to that in the line.

The equations (4) were transformed into the optical depth scale where

$$d\tau = K_L(z) dz = \frac{h\nu_0}{4\pi \Delta} (n_l(z) B_{lk} - n_u(z) B_{ul}) dz \quad (5)$$

$\Delta$ , being the Doppler width is equal to  $\frac{v_0}{c} \left( \frac{2kT}{m} \right)^{1/2}$ .

$n_1(z)$  and  $n_2(z)$  are the number densities of the lower and upper levels of the transition.

The source function  $S(x, \pm\mu, z)$  is given by

$$S(x, \pm\mu, z) = \frac{\phi(x, \pm\mu, z) S_L(x, \pm\mu, z) + \beta S_c(z)}{\phi(x, \pm\mu, z) + \beta} \quad (8)$$

$S_L$  and  $S_c$  refer to the source function in the line and continuum respectively.  $\phi(x, \mu, z)$  is the profile function. Complete redistribution with Voigt profile function  $H(a, x)$  was assumed. When there is velocity field, the frequency of the line photon is shifted by

$$x - x' + v(\tau) \mu \quad (7)$$

Where  $V(\tau)$  is the velocity of the gas in mean thermal units at the point  $\tau$ . Line source function for a multi-level atom for the transition between the lower level 1 to the upper level  $u$  is given by (Mihalas, 1978)

$$S_{1u} = \left[ \int \phi_{\nu} J_{\nu} dx + (\epsilon + \theta) B_{\nu}(T_e) \right] / (1 + \epsilon + \eta) \quad (8)$$

where  $\epsilon$  gives the number of photons that are destroyed by collisional deexcitation following photoexcitation and is defined by

$$\epsilon = C_{u1} \left( 1 - e^{-h\nu/kT} \right) / A_{u1} \quad (8)$$

The effects on radiation field due to other lines is described by terms  $\eta$  and  $\theta$ . They are described by

$$\eta = [a_2 a_3 - (g_1/g_u) a_1 a_4] / [A_{u1} (a_2 + a_4)] \quad (10)$$

$$\theta = \left[ \sum_{l < j \neq u} n_l a_{jl} \left( 1 - e^{-h\nu/kT} \right) \right] / [n_u A_{u1} (a_2 + a_4)] \quad (11)$$

where

$$a_1 = R_{1k} + C_{1k} + \sum_{l < 1} A_{1l} Z_{1l} + \sum_{l < j \neq u} C_{1j} Y_{1j}$$

$$a_2 = n_1 (R_{k1} + C_{1k}) + \sum_{l < j \neq u} n_j A_{jl} Z_{j1} + \sum_{l < 1} a_l C_{1l} Y_{11}$$

$$a_3 = R_{u1} + C_{u1} + \sum_{u > j \neq 1} A_{uj} Z_{uj} + \sum_{u < j} C_{uj} Y_{uj}$$

$$a_4 = n_u (R_{ku} + C_{uk}) + \sum_{u < j} n_j A_{ju} Z_{ju} + \sum_{u > j \neq 1} n_j C_{ju} Y_{ju}$$

and the net radiative bracket  $Z_{jl}$  and the net collisional bracket  $Y_{ij}$  are defined by

$$Z_{jl} = 1 - \bar{J}_{ij} (n_i B_{ij} - n_j B_{ji}) / n_j A_{ji} \quad (13)$$

$\bar{J}_{ij}$  being the mean intensity in the line and  $B_{ji}$ ,  $B_{ij}$  are the Einstein emission and absorption coefficients respectively.

$$Y_{ij} = 1 - \frac{n_i}{n_l} \frac{C_{ji}}{C_{ij}} \quad (14)$$

The statistical equilibrium equations for a multi-level atom are given by

$$n_l \left( \sum_{u=1}^M (B_{lu} \bar{J}_{lu} + C_{lu}) + R_{lk} + C_{lk} \right) - \sum_{v=1}^M n_v (A_{vl} + B_{vl} \bar{J}_{lv} + C_{vl}) + n_k (R_{kl} + C_{kl}) = \sum_{l=1}^M n_l + n_k = N \quad (15)$$

here  $N$  is the number of  $\text{Ca}^+$  ions, and  $M$  is the number of levels considered.

We divided the medium into 5 shells. Velocity at each shell is given by

$$V(\tau) = V(A) + \left( \frac{V(B) - V(A)}{N} \right) \times n$$

here  $A, B$  are the inner and outer radii of the atmosphere.  $n$  denotes the number of the shell and  $N$  is the total number of layers. We have set  $V(A) = 0$  and  $V(B) = 0, 0.5$  and  $1$ .  $\beta$  was taken to be zero. Damping parameter 'a' was assumed to be  $10^{-3}$ . We solved equations (4) and (15) with the following boundary conditions:

1. Incident radiation at the top of the atmosphere was zero. The incident radiation at the lower layer of the atmosphere was assumed to be  $B\nu$  ( $T_e = 4620$  K)

2. Above equations were solved iteratively. We chose LTE number densities to be initial values for calculating the optical depth from the relation (6). To calculate the radiation field in any line,  $\theta$  and  $n$  have to be specified which depend on the radiation field of other lines. To compute the H-line radiation field, we assumed radiation field in other lines to be Planckian. While computing the K-line, we substituted the computed H-line densities, keeping the unknown radiation fields in infrared triplet lines as Planckian. This procedure was continued till the intensities of all the five lines were calculated.

To get the number densities in the levels, we substituted mean intensities of all the five lines in the statistical equilibrium equations. This new number densities were used to calculate the optical depth. Since we know radiation field in all the lines, we substituted those values to compute the intensities of all the lines second iteration. Iterations were continued till the number densities converged up to a deviation of less than 1% of the previous iteration values.

## Results

Emergent intensities of K line for the various velocities when  $\mu = 0.79$  are plotted in figure 4. The total optical depth at the line centre was 618. We find a symmetric profile with a double peaked emission for the static case and for non zero velocities, we find a blue shift and asymmetry in the profiles. When the velocity at the outer boundary is one mean thermal unit, only a single peak in the red side ( $K_{2r}$ ) with a blue shift of a minimum was obtained.  $K_2$  absorption feature broadens with velocities. A similar trend is seen in the limb ( $x=0.21$ ) also (fig.5). We also find  $K_{2r} > K_{2v}$  when  $V=0.5$ . The emergent flux profiles for the above velocities are plotted in fig. 6. Asymmetry is more pronounced in the flux profiles.

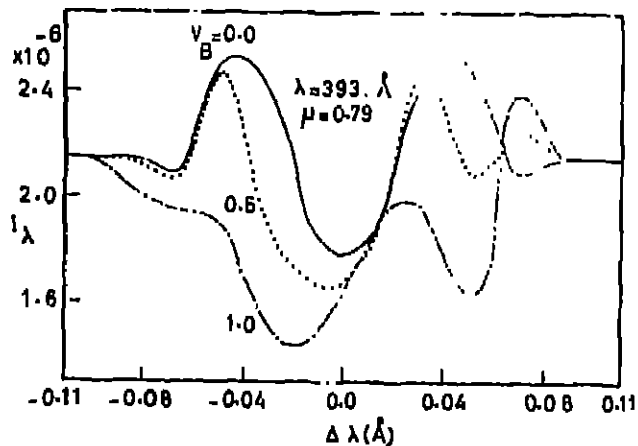


Fig. 4. Ordinate: Emergent Intensity  $I_{\lambda}$  ( $\text{ergs cm}^{-2} \text{\AA}^{-1} \text{ster}^{-1} \text{sec}^{-1}$ ) of K line ( $3933 \text{\AA}$ ) for  $\mu=0.79$  and velocities  $V=0.0$ ,  $0.5$  and  $1$  Absoless. Displacement  $\Delta\lambda$  from the line centre in  $\text{\AA}$ .

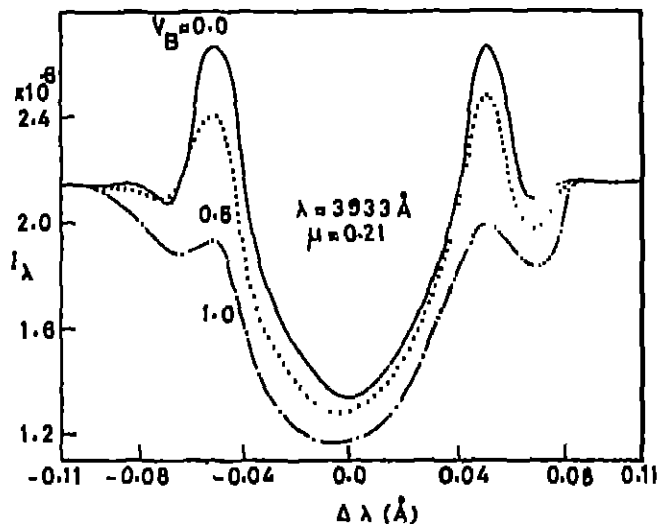


Fig. 5. Same as that in fig. 4 with  $\mu=0.21$ .

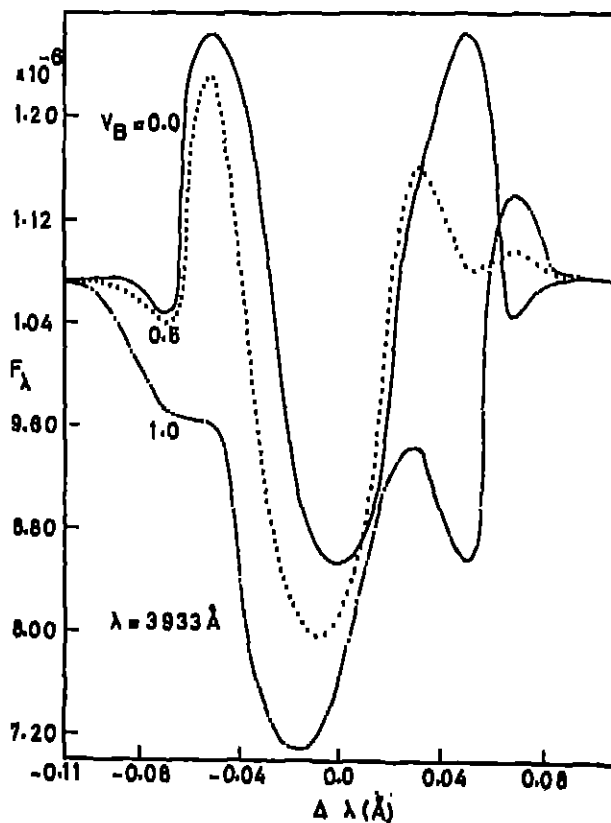


Fig. 6. Ordinate: Emergent flux  $F_{\lambda}$  ( $\text{ergs cm}^{-2} \text{\AA}^{-1} \text{sec}^{-1}$ ) of K line for velocities,  $V=0.0$ ,  $0.5$  and  $1.0$  Absoless. Displacement from line centre in  $\text{\AA}$ .

Emergent intensities of H line at  $\mu=0.79$  for various velocities are plotted in figure 7. H line intensities are consistently higher than K line intensities. This is due to the lesser optical depth of H line which is only 322. Both H and K lines exhibit similar trends. Narrow emission peaks occur for  $V=0.5$ . Emergent intensities of 8662 line for  $\mu=0.79$  and 0.21 are given in figures 10 and 11. Figures 12 and 13 show the emergent intensities of the line 8542 for  $\mu=0.79$  and 0.21 respectively. Emergent intensity profiles of 8498 are plotted in figures 14 and 15.

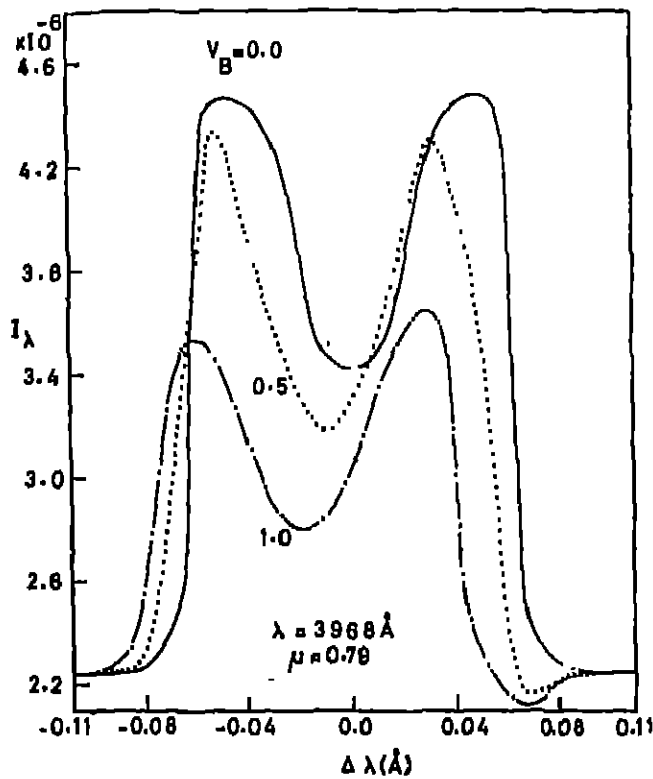


Fig. 7 Same as in fig. 4 for H line (3968 Å).

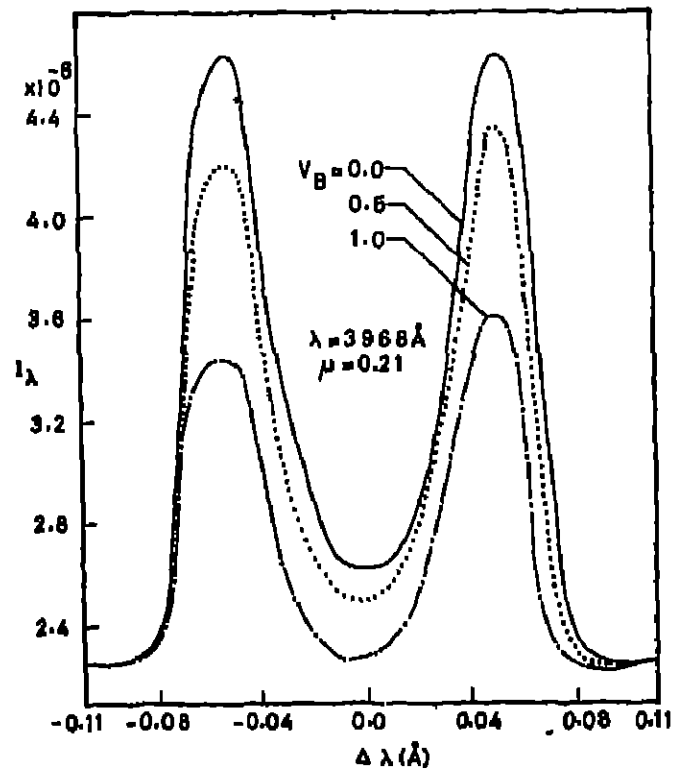


Fig. 8 Same as in fig. 7 with  $\mu = 0.21$ .

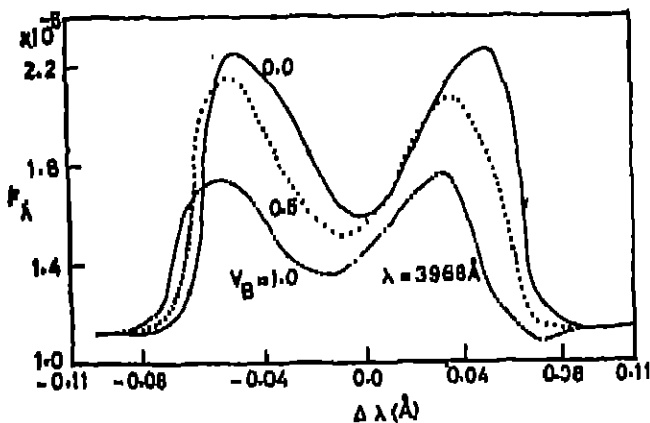


Fig. 9 Same as in fig. 6 of H line.

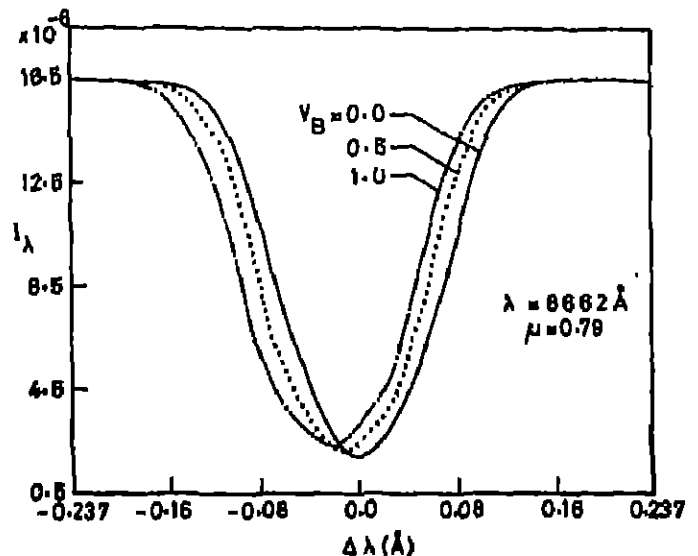


Fig. 10 Same as in fig. 4 for the infrared triplet line 8662 Å.

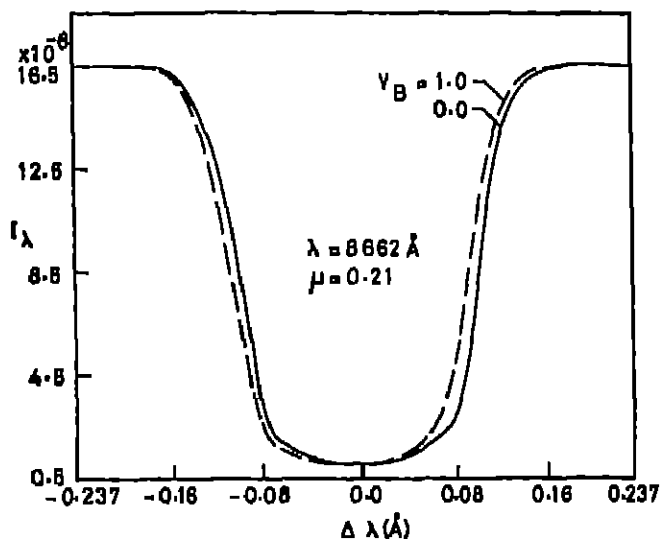


Fig. 11 Same as in fig 10 with  $\mu=0.21$  and for velocities  $v_B = 0.0$ , and 1.0 only.

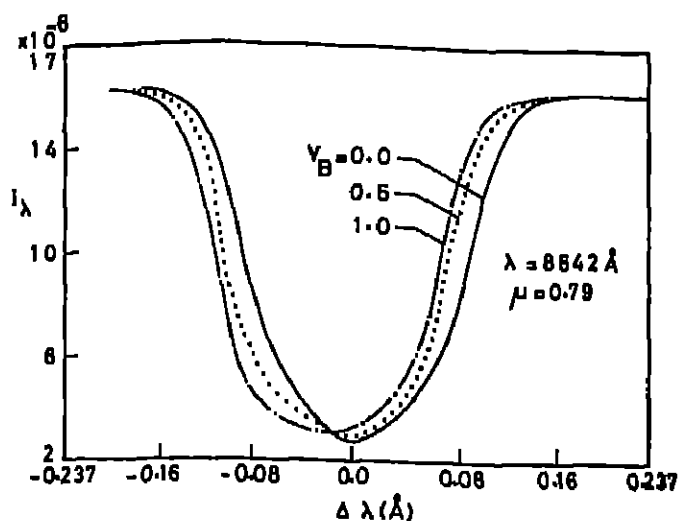


Fig. 12 Same as in fig. 10 for 8642 Å.

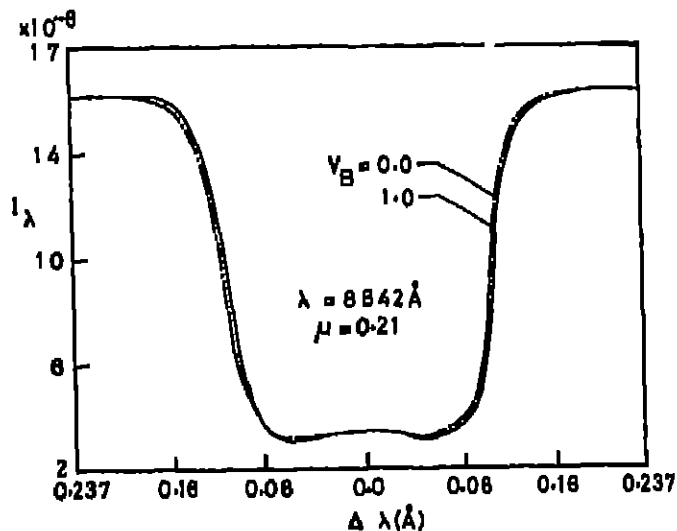


Fig. 13 Same as in fig. 12 with  $\mu=0.21$  and for  $v_B = 0.0, 1.0$ .

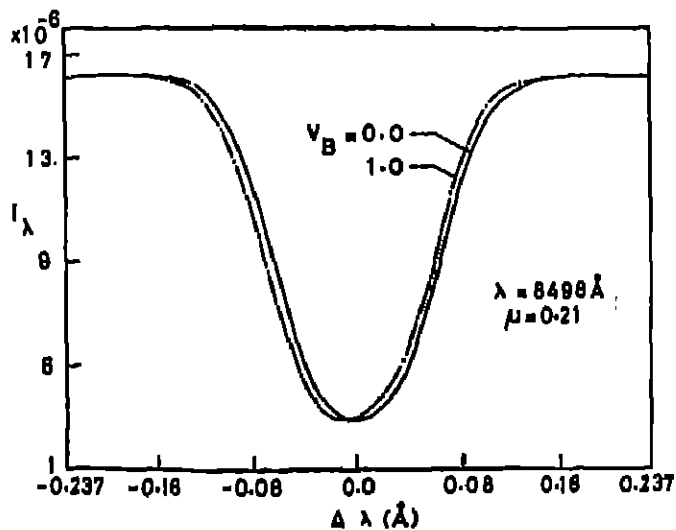


Fig. 15 Same as in fig. 14 with  $\mu=0.21$  and for  $v_B = 0.0, 1.0$  only.

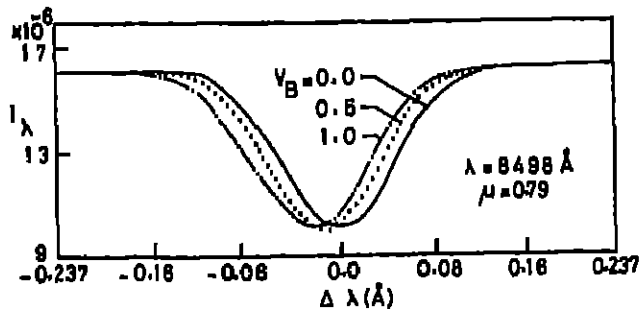


Fig. 14 Same as in fig. 10 for 8498 Å line.



All the Infrared triplet lines have deep absorption profiles except for 8498 line at  $\mu = 0.79$ . This line is the weakest due to the least optical depth at the line centre. With velocities, we find all the lines to be blue shifted. Near the limb the velocity effects on the line profiles are negligible.

### Conclusion

With the chosen model atmosphere, we find double peaked emission for H and K lines in the static medium. Our results show that the systematic velocity fields do play a significant role in determining the shape of the H and K profiles. The small velocities did not affect the Infrared triplet lines significantly. When there is a velocity towards the observer of the order of  $2.13 \text{ km s}^{-1}$  in the K line, only a single peaked emission on the red side ( $K_2$ ) and a blue shift of the  $K_3$  minimum were obtained.

For matching the theoretical results with the observations one has to consider a more realistic model atmosphere. The effects of spherical geometry and the angle dependent partial frequency redistribution functions on the line transfer have to be investigated especially for the cool super giants.

### Reference

- Athay G R. 1970. *Sol. phys.* 11, 347.  
 Basri, G.B., Linsky, J.L., Eriksson, K. 1981, *Astrophys. J.*, 251, 162.  
 Dumont, S. 1867, *Annales d' Astrophysique*, 30, 421.  
 Glovanelli, R.G. 1967, *Australian J. Phys.*, 20, 81.  
 Grant, I P., Peralah, A. 1972, *Mon. Not. R. astr. Soc.*, 160, 239.  
 Linsky, J.L., 1968, *Smithsonian Astrophys. Obs. Spec. Rep.*, No. 274.  
 Linsky, J.L., Avrett, E.H. 1970, *Publ. Astr. Soc. of Pacific*, 82, 169.  
 Mihailes, D. 1978, *Stellar Atmospheres*. 2nd ed., W.H. Freeman & Co., San Francisco.  
 Pasachoff 1970. *Solar Phys.*, 12, 202.  
 Posch, G. 1867, *Mem. Royal Astr. Soc.*, 71, 1.  
 Peralah, A. 1978, *Kodaiikanal Obs. Bull. Ser. A. 2*, 115.  
 Shino, R.A., Milkey, R.W., Mihailes, D. 1975, *Astrophys. J.*, 199, 724.